arXiv:cond-mat/0311635v1 [cond-mat.soft] 27 Nov 2003

First order isotropic - smectic-A transition in liquid crystal-aerosil gels

M.K. Ramazanoglu, P.S. Clegg, and R.J. Birgeneau
Department of Physics, University of Toronto, Toronto, Ontario M5S 1A7, Canada

C.W. Garland
Department of Chemistry, Massachusetts Institute of Technology, Cambridge, MA 02139

M.E. Neubert and J.M. Kim
Liquid Crystal Institute, Kent State University, Kent, Ohio, 44242

(Dated: February 2, 2008)

The short-range order which remains when the isotropic to smectic-A transition is perturbed by a gel of silica nanoparticles (aerosils) has been studied using high-resolution synchrotron x-ray diffraction. The gels have been created *in situ* in decylcyanobiphenyl (10CB), which has a strongly first-order isotropic to smectic-A transition. The effects are determined by detailed analysis of the temperature and gel density dependence of the smectic structure factor. In previous studies of the continuous nematic to smectic-A transition in a variety of thermotropic liquid crystals the aerosil gel appeared to pin, at random, the phase of the smectic density modulation. For the isotropic to smectic-A transition the same gel perturbation yields different results. The smectic correlation length decreases more slowly with increasing random field variance in good quantitative agreement with the effect of a random pinning field at a transition from a uniform phase directly to a phase with one-dimensional translational order. We thus compare the influence of random fields on a *freezing* transition with and without an intervening orientationally ordered phase.

PACS numbers: 64.70.Md,61.30.Eb,61.10.-i

I. INTRODUCTION

The formation of the smectic-A (SmA) phase is intriguing because the resulting one-dimensional density modulation lacks true long-range order [1, 2]. Much effort has been devoted to experimental characterization and theoretical description of the SmA phase of thermotropic liquid crystals [3, 4]. More recently, the effects of quenched random disorder on the nematic (N) - SmA transition have been studied. The interplay between the thermal fluctuations which disrupt the long-range order and static fluctuations due to quenched randomness is fascinating. Experimentally, quenched randomness can be introduced via a porous random environment such as aerogel. In order to probe weaker disorder the rigid aerogel has been replaced by a hydrogen-bonded gel of aerosil particles. In both cases the N - SmA transition has been studied using calorimetry [5, 6], deuterium NMR [7, 8] and x-ray diffraction [9, 10]. In addition, results have been presented for the isotropic (I) - SmA transition for a liquid crystal confined in an aerogel [11]. Here we present a comprehensive x-ray diffraction study for an aerosil gel.

For many liquid crystals the SmA phase forms from the orientationally ordered N phase. There is coupling between the order parameters and fluctuations of the two phases. As the SmA phase becomes more favorable at higher temperatures, due to changes in the molecule or mixture composition, the N-SmA transition occurs while the N order parameter is less and less saturated. The transition into the SmA phase enhances the N order. This coupling between order parameters leads to a tricritical point in the phase diagram [12]. As the stability of the SmA phase is further enhanced a triple point occurs in the phase diagram and the N phase ceases to be stable. Beyond this point, orientational order occurs along with positional order in the SmA structure. The pretransitional fluctuations of the SmA order in the I phase occur over a sphere of ordering wave vectors corresponding to the layer spacing. The transition is thought to be first order due to the contribution of these fluctuations as described by Brazovskii [13, 14]. The observation that the I-SmA transition is strongly first order for 10CB [15, 16] may well be due to the de Gennes coupling between smectic and nematic order parameters in the isotropic phase [17].

The cyanobiphenyls are a well-studied family of thermotropic liquid crystals [18]. These molecules have a flexible aliphatic tail the length of which influences the stability of the SmA phase. Both decylcyanobiphenyl (10CB) and dodecylcyanobiphenyl (12CB) exhibit transitions directly from the I phase to the SmA phase. Since, in establishing the SmA order, both orientational and positional order must be developed, one might expect this transition to be especially strongly perturbed by quenched random disorder. Thixotropic (hydrogen bonded) gels can be created by dispersing fine, hydrophilic aerosil particles in the liquid crystal. These silica nanoparticles hydrogen bond together creating a flexible structure which can substantially perturb the interpenetrating liquid crystal material. The pore volume fractions range from 0.77 to 0.99.

Previous studies of the N-SmA transition in liquid crystal-aerosil gels have implied that the main effect of the aerosils is to pin the phase of the SmA density

wave [10, 19, 20]. Specifically, both the size of the SmA domains and the detailed wave vector dependence of the x-ray structure factor have been in quantitative agreement with the predictions of a random pinning field model. In this paper we are reporting the results of a study of the random field model at a first-order transition. As first articulated by Imry and Ma, the simplest understanding of the effects of random fields comes from considering a balance between the benefit of aligning with the local random field and the cost of forming a domain wall [21]. This model predicts differing responses for transitions which break discrete and continuous symmetries. The situation becomes more complicated for first-order transitions due to the possibility of two-phase coexistence [22]. Domain walls can exist between ordered and disordered regions as well as between ordered domains. A guide to the likelihood of two-phase coexistence is whether the disorder causes a substantial suppression of the phase transition temperature. Should it do so, it is likely that *large* variations of transition temperatures will occur locally giving two-phase coexistence so that the sharp transition will then be smeared out. Two-phase coexistence will alter the penalty for forming domain walls. Substantial two-phase coexistence results in sharp boundaries between ordered and disordered regions. This has similarities to a transition which breaks a discrete symmetry with random fields. One might speculate that long-range order could be observed for sufficiently weak disorder in $d = 3$. Without significant two-phase coexistence the domain walls will be broad and the response should correspond to expectations for a transition which breaks a continuous symmetry in the presence of random fields.

In reference [11] a silica aerogel is used to impose quenched disorder on 10CB, and similar previous studies of the liquid crystal 650BC are also discussed. Both of these materials exhibit transitions directly from the I to the SmA phase. The correlation lengths are observed to increase discontinuously at the transition temperature and to saturate quickly. Meanwhile, the scattering intensity increases only slowly with decreasing temperature. The transition is observed to remain first order under this strong confinement and this is confirmed via optical microscopy of the coexisting phases. It is surprising that the correlation length remains almost constant as the SmA order goes from the two phase coexistence region to the uniform phase region. The transition temperature is found to remain roughly unchanged.

Here we show that the liquid crystal-aerosil gel also retains only short-range SmA order deep into the SmA phase temperature region. In common with previous studies, a range of gel densities have been prepared and characterized using high-resolution x-ray diffraction. The results demonstrate that our quantitative understanding of the N-SmA transition naturally extends to this new class of transition. In Sec. II we outline preliminary details including the differences for x-ray diffraction between the I-SmA transition and the N-SmA transition and the experimental techniques employed. Section III gives the results and analysis. The quantitative comparison between these results and existing theoretical models is discussed in Sec. IV and conclusions are drawn.

II. PRELIMINARY DETAILS

A. X-ray Structure Factor

The x-ray scattering line shape approaching the N-SmA transition [23] and deep within the SmA phase [24] have been characterized in great detail. In the former case the data for a wide range of liquid crystalline materials have been found to be described by the structure factor

$$S(\mathbf{q}) = \frac{\sigma_0}{1 + \xi_\parallel^2 (q_\parallel - q_0)^2 + \xi_\perp^2 q_\perp^2 + c\xi_\perp^4 q_\perp^4} \qquad (1)$$

where $q_0 = 2\pi/d$ is the wave vector where the SmA peak occurs corresponding to a layer spacing d. The correlation length $\xi_\parallel(\xi_\perp)$ and wave vector components $q_\parallel(q_\perp)$ are parallel (perpendicular) to the nematic director. The susceptibility is σ_0, while c ranges between 0.25 and 0 and gives the scale of the fourth-order correction. The second-order $q_\perp$ contribution to the line shape arises due to the influence of nematic fluctuations on the formation of the SmA state [25]. Far below the N-SmA transition these fluctuations are constrained to be perpendicular to the smectic layers. In the case of finite correlation lengths, $\xi_\parallel$ and $\xi_\perp$, the structure factor then can be written approximately as

$$S(\mathbf{q}) = \frac{\sigma_0}{1 + \xi_\parallel^2 (q_\parallel - q_0)^2 + \xi_\perp^4 q_\perp^4} \qquad (2)$$

In the case of infinite correlation lengths, the structure factor has been described by Caillé [26] and varies with $(q_\parallel - q_0)^{-2+\eta}$ and $q_\perp^{-4+2\eta}$ respectively (η depends on the elastic constants) [24].

Experimental determination of these structure factors for pure liquid crystals was carried out in an applied magnetic field. In the N phase all regions of the sample become aligned allowing detailed characterization of the pretransitional smectic fluctuations or the algebraic decay within the SmA state. Equivalent studies are not possible for the I-SmA transition since there is no possibility of magnetic field alignment in the N state. Hence, only very preliminary studies have been made of the line shape for 12CB [27]. In what follows, we analyze our results assuming that the SmA fluctuations are either similar to those in nonylcyanobiphenyl (9CB) as given by Eq.(1) or that the scattering is described by Eq.(2). At the I-SmA transition the orientational order is caused by the formation of the SmA state. As a result, we anticipate that the nematic director will be constrained to lie perpendicular to the smectic layers. By this argument Eq.(2) appears to be a good approximation to the structure factor.

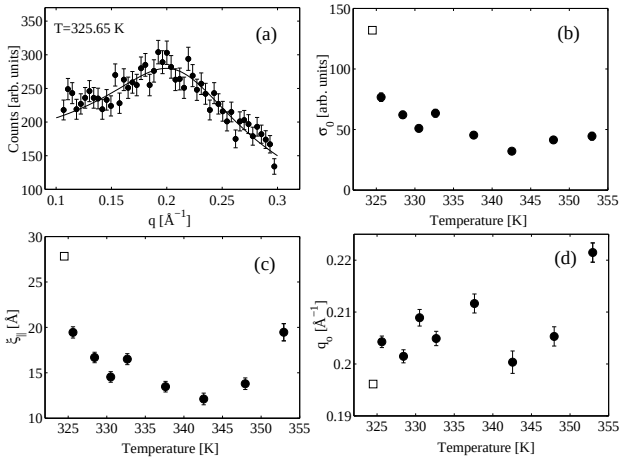

FIG. 1: Measurements and analysis of pretransitional smectic fluctuations in bulk 10CB. Panel (a) shows a typical scan of the scattering intensity versus wave-vector transfer. The solid line is the result of a fit with Eq.(1). Panels (b, c, d) show susceptibility, parallel correlation length, and peak position resulting from fits to the data. The open symbol is in the region of coexistence of isotropic and smectic phases.

B. Experimental Techniques

The 10CB was synthesized at Kent State University. Type-300 aerosil was supplied by Degussa [28] and was dried prior to use. The amount of aerosil in each sample was quantified by the parameter ρ_S, the mass of aerosil divided by the volume of liquid crystal. X-ray diffraction experiments were carried out at the National Synchrotron Light Source at Brookhaven National Laboratory. The beam lines used were X20A, X20C and X22A. Liquid crystal samples containing dispersed aerosils were in the solid phase following long periods at room temperature and so prior to study were remixed with pure ethanol, sonicated and then dried for several days on a hot plate. The gel samples were placed in 5-mm radius disks which have kapton windows [29]. The kapton x-ray diffraction signal has a powder peak outside the range of interest for these experiments. Temperature control is via a PI controller to within ± 0.05 K. Each sample was kept in the I phase at a temperature around 30 K above the I-SmA transition for 6 hours after being transferred to the holder. The number of scans for each sample was kept limited to avoid undue x-ray damage.

III. RESULTS AND ANALYSIS

Figure 1 presents our measurements and analysis of the pretransitional fluctuations in the isotropic phase of 10CB. Pretransitional smectic fluctuations are extremely weak in the pure material and were never evident in the gel samples. Figure 1(a) shows a typical scan; the peak is very broad and the solid line is the result of a fit to Eq.(1) varying σ_0, q_0, and $\xi_{\parallel}$ and using the known 9CB characteristics for $\xi_{\perp}(\xi_{\parallel})$ and $c(\xi_{\parallel})$. The parameters from such fits are displayed in panels b,c,d of Fig. 1. There is no indication that the susceptibility, σ_0, or the parallel correlation length, $\xi_{\parallel}$ are about to diverge. The weakness of the fluctuations immediately prior to the transition strongly suggest that this is not a typical fluctuation driven first-order transition. The observed behavior is likely due to the de Gennes coupling between nematic and smectic order parameters.

The 10CB-aerosil sample compositions studied are listed in Table I. Measurements were made from a temperature ($T \sim 350$ K) well above the I-SmA transition ($T_{IA} = 324.5$ K). However, the SmA line shape for 10CB-aerosil samples only appeared at a pseudotransition temperature with a substantial correlation length already established. Typical scans are presented in Fig. 2. The peaks are all broader than the instrumental resolution. The width increases with increasing gel density but varies little with temperature. Data were taken down to $T = 298$ K, which is well below the bulk material crystallization temperature [30] ($T_K = 317.1$ K). The lines in Fig. 2 corresponds to a model that will be described below. Two samples, $\rho_S = 0.025$ and 0.282, were measured on beam-line X22A where slightly higher instrumental resolution could be achieved. Typically, the peak position in the SmA phase was $q_0 = 0.1776$ Å^{-1}, rising just below the transition and dropping slightly at lower temperatures.

For previous x-ray studies of the N-SmA transition in aerosil gels, the line shape was taken to be composed of two contributions [10, 20, 29, 31]. The first part is the thermal term, Eq.(1), which is identical to that of the pure material, while the second part is the random-field term, which has the form of the thermal term squared.

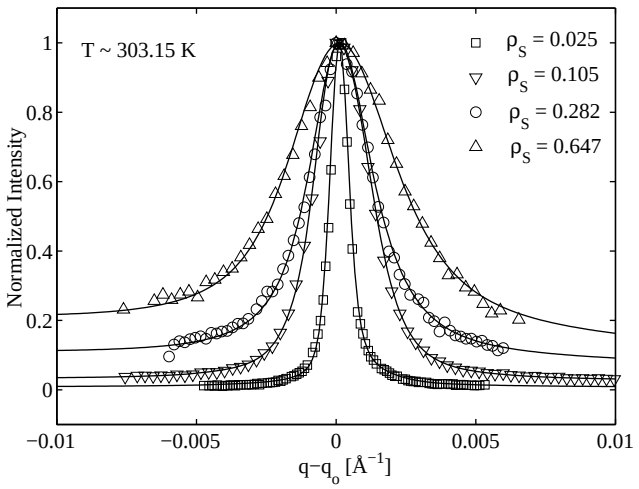

FIG. 2: Normalized x-ray scattering intensity versus wave-vector transfer for 10CB-aerosil gels due to short-range SmA order at a temperature ~ 20 K below the effective T^*_{IA} value. The lines are the results of fits with a model described in the text.

The total structure factor is

$$S(\mathbf{q}) = \sigma_1 S^T(\mathbf{q}) + S^{RF}(\mathbf{q}) \quad (3)$$
$$S^{RF}(\mathbf{q}) = a_2(\xi_\parallel \xi_\perp^2)[S^T(\mathbf{q})]^2$$

where $S^T(\mathbf{q})$ corresponds to Eq.(1) for the N-SmA transition with the numerator set equal to 1 and the denominator of $S^{RF}(\mathbf{q})$ is the square of the denominator of $S^T(\mathbf{q})$. σ_1 and a_2 are the amplitudes for the thermal and random-field terms respectively. Since the samples are comprised of a random arrangement of ordered domains this structure factor has to be averaged over all orientations. Prior to comparing the model with the data this spherically averaged line shape must be convoluted with the measured instrumental resolution function. Both the integral over orientations and the convolution were performed numerically using commercially available routines.

Figure 3 shows the results of fits to a typical profile. The dotted and solid lines result from applying Eq.(3) to the 10CB-aerosil data using the form of Eq.(1) for $S^T(\mathbf{q})$. Here, as elsewhere [10, 20, 29, 31], we take $\xi_\parallel$ as a parameter to be fitted and we assume that $\xi_\perp(\xi_\parallel)$ and $c(\xi_\parallel)$ remain the same as for the pure material [32]. The behavior of $\xi_\parallel$, $\xi_\perp$ and c for 10CB are not known. The dotted and the solid line in Fig. 3 assume that 8CB behavior and 9CB behavior for $\xi_\perp(\xi_\parallel)$ and $c(\xi_\parallel)$ are followed respectively [33]. It is evident that either fit gives a reasonable description of the data, with the use of 9CB parameters yielding a somewhat better fit. **This model using the 9CB relationships for $\xi_\perp(\xi_\parallel)$ and $c(\xi_\parallel)$ has been used to analyze all of the 10CB-aerosil results.** The fit parameters are q_0, σ_1, a_2, and $\xi_\parallel$, whose optimum values are determined using a least-squares fitting procedure. The dashed line in Fig. 3 shows the result of a fit with Eq.(3) to the 10CB-aerosil data using the form of Eq.(2) for $S^T(\mathbf{q})$. Again $\xi_\perp(\xi_\parallel)$ is assumed to remain the same as in bulk 9CB; however in this case the transverse tails of the peak are assumed to have changed. This model also gives a good correspondence to the data. Use of a model based on Eq.(2) for the form of $S^T(\mathbf{q})$ systematically modifies the fit parameters compared to those presented here. There is a small shift in favor of the thermal term and the correlation length decreases. The latter feature is returned to in more detail below.

The variation of the two components of the line shape, with temperature and ρ_S is shown in Fig. 4. Panels Fig. 4(a & b) are for high temperature and Fig. 4(c & d) are for low temperature. While Fig. 4(a & c) are for low ρ_S and Fig. 4(b & d) are for high ρ_S. The second term in Eq.(3) dominates the scattering for all temperatures studied (dashed line). The full model Eq.(3) using Eq.(1) for $S^T(\mathbf{q})$ is the solid line. The peak width varies little with temperature but is seen to be broader than the instrumental resolution (Fig. 4).

Figures 5 and 6 show parameters determined by the fit procedure versus temperature while Figs. 7 and 8 show parameters versus ρ_S. In the latter case, the results are compared to those from other liquid crystal-aerosil gels at temperatures below the N-SmA transition.

The behavior of the parallel correlation length, $\xi_\parallel$, as a function of temperature is shown for a selection of samples in Fig. 5 (solid symbols). The fact that these are all finite shows that the quasi long-range SmA state has been destroyed by the gel. The pseudotransition to short-range smectic order remains sharp and the correlation length jumps directly to its low temperature value with no pretransitional fluctuations. This behavior strongly suggests that the transition remains first order in the gels. As the gel density is increased the correlation length systematically decreases. The open symbols in Fig. 5 show the values for $\xi_\parallel$ determined using Eq.(3) with Eq.(2) for $S^T(\mathbf{q})$. The systematic decrease in $\xi_\parallel$ results from the narrower transverse profile of Eq.(2) for a particular $\xi_\perp$

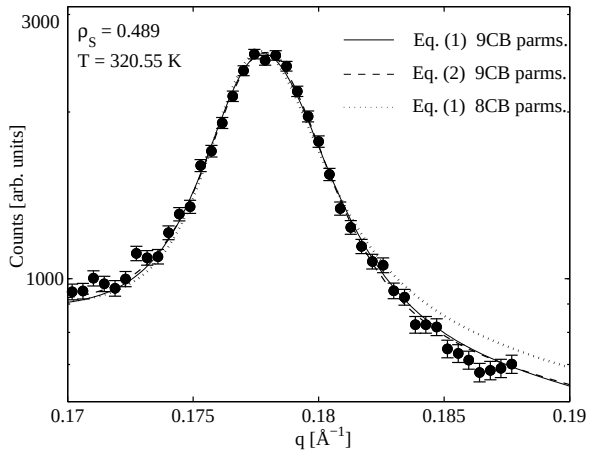

FIG. 3: X-ray scattering intensity due to SmA correlations. The three lines represent three different models where the assumptions have been changed. The models and the assumptions are described in the text.

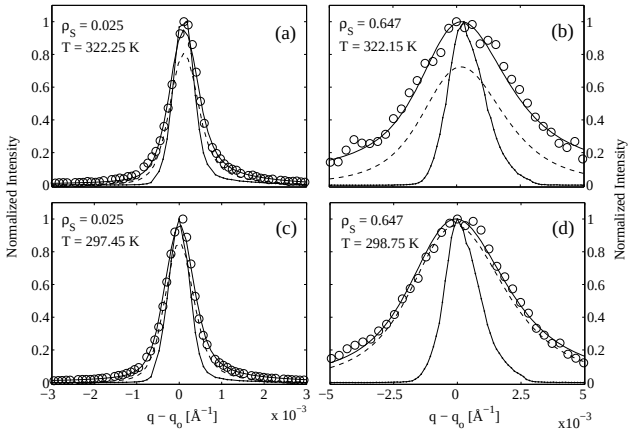

FIG. 4: The variation in the random field contribution (dashed line) to the x-ray scattering intensity (open circles) with temperature and ρ_S. The experimental resolution corresponding to each scan is shown as dots joined by a solid line.

TABLE I: Parameters for bulk 10CB and eight gel samples. Shown are the density, ρ_S, the mass of aerosil per unit volume of liquid crystal; the pore volume fraction Φ; the low temperature parallel correlation length $\xi_\parallel$; the low-temperature ratio of the random-field amplitude a_2 to the thermal amplitude σ_1; the pseudotransition temperature T^*_{IA}, and the exponent x describing the temperature dependence of a_2.

ρ_S (g cm^{-3})	Φ	$\xi_\parallel$ (Å)	a_2/σ_1 ($\times 10^{-6}$Å^{-3})	T^*_{IA} (K)	x
0.0	1	-	-	324.49	-
0.025	0.99	4786 ± 85	0.071 ± 0.003	323.6 ± 0.4	0.14 ± 0.01
0.051	0.98	1927 ± 24	1.13 ± 0.05	323.8 ± 0.8	0.19 ± 0.03
0.105	0.95	1396 ± 9	1.74 ± 0.04	323.2 ± 0.2	0.39 ± 0.15
0.226	0.91	806 ± 8	10.8 ± 0.9	323.8 ± 0.1	0.22 ± 0.02
0.282	0.89	804 ± 29	2.35 ± 0.30	323.0 ± 0.1	0.32 ± 0.06
0.355	0.86	641 ± 6	12.2 ± 0.9	323.6 ± 0.3	0.51 ± 0.20
0.489	0.82	445 ± 9	40.3 ± 20.4	323.5 ± 0.3	0.39 ± 0.10
0.647	0.77	543 ± 24	7.62 ± 2.99	322.7 ± 0.1	0.41 ± 0.13

value. Since the shifts are approximately equal on a logarithmic scale this result does not modify any of the power law relationships discussed in Sec. IV.

The corresponding temperature dependence of the amplitude of the random-field term, a_2, is shown in Fig. 6 for three samples. The temperature dependence is consistent with the random field fluctuations increasingly dominating the scattering at low temperatures. In Sec. IV we will discuss the difference between the behaviors of $a_2(T)$ and $\xi_\parallel(T)$. In contrast to the correlation length behavior, the growth of this amplitude parameter becomes increasingly more gradual as ρ_S increases. As with N-SmA transitions in aerosil gels [29], $a_2(T)$ can be compared to an order parameter squared for the pseudotransition. The lines in Fig. 6 are the results of fits with the form $a_2 \sim (T^*_{IA} - T)^x$. We emphasize that this form, which is normally used at a second-order transition with $x = 2\beta$, is used here to provide a strictly phenomenological description of the data. The inset in Fig. 6 shows the x values, and both they and the resulting pseudotransition temperatures, T^*_{IA}, are presented in Table I. Although there is substantial scatter, the x values indicate that a_2 is growing more gradually with increasing ρ_S.

Figure 7 shows a log-log plot of the variation of the smectic domain size with the gel density, ρ_S. The smectic domain size is quantified by an isotropic correlation length $\overline{\xi} = (\xi_\parallel \xi_\perp^2)^{1/3}$ and the low-temperature average of this quantity is shown. The line through the 10CB-aerosil data corresponds to $\overline{\xi} \sim \rho_S^{-1/2}$. Also plotted in Fig. 7 are $\overline{\xi}$ results for 8CB-aerosil [10] and 8OCB-aerosil [20] samples, for which $\overline{\xi} \sim \rho_S^{-1}$. This contrast will be discussed in Sec. IV.

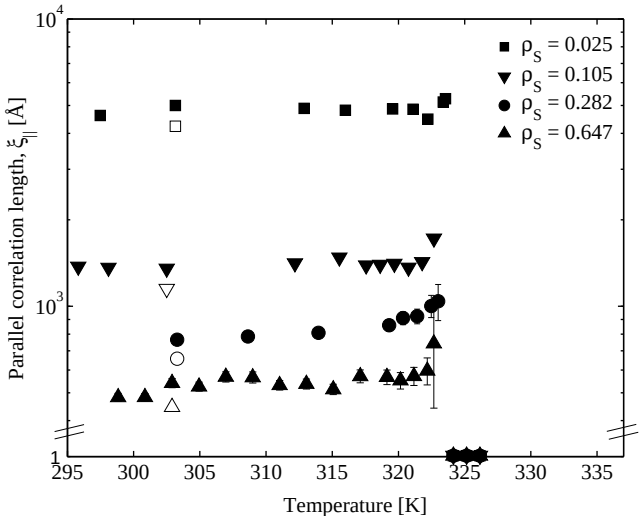

FIG. 5: The parallel correlation length, $\xi_\parallel$, for smectic order as a function of the temperature for four 10CB-aerosil samples. These values denoted by solid symbols are determined using Eq.(1) for $S^T(\mathbf{q})$ in Eq.(3) while the four open symbols correspond to substituting for $S^T(\mathbf{q})$ given by Eq.(2) into Eq.(3).

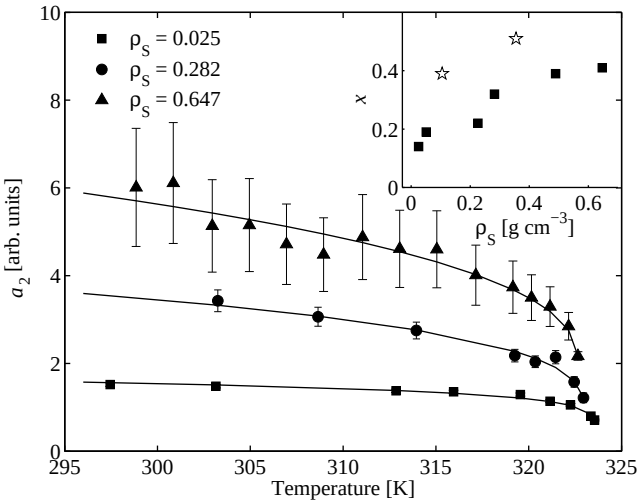

FIG. 6: Integrated intensity of the random-field term $S^{RF}(\mathbf{q})$ versus temperature. The solid lines are the results of fits to a $(T^*_{IA} - T)^x$ power law form. The x values are shown in the inset and in Table I along with the pseudotransition temperatures. The stars in the inset indicate the most uncertain x values.

Figure 8 is a log-log plot of a_2/σ_1 versus the disorder strength as represented by ρ_S. This ratio gives the strength of the random-field contribution to the scattering and is independent of x-ray intensity normalization. Equivalent values are plotted for 8CB-aerosil [10] and 8OCB-aerosil [20] samples. While the scatter is rather large, the results are consistent with power law behavior with $a_2/\sigma_1 \sim \rho_S^3$ for N-SmA and $a_2/\sigma_1 \sim \rho_S^{3/2}$ for the I-SmA. The low temperature values of a_2/σ_1 and $\xi_\parallel$ are included in Table I. These are the mean values below 315 K.

IV. DISCUSSION AND CONCLUSIONS

Our results show that an aerosil gel reduces the SmA state to short-range order with random-field characteristics. At first sight, the temperature dependencies in Fig. 5 and 6 are a little surprising. The behavior of the correlation length, $\xi_\parallel$, suggests a first-order transition for all ρ_S while the random-field amplitude, a_2, suggests an increasingly gradual transition with increasing ρ_S. For pure 10CB the pretransitional fluctuations are very weak and short range, Fig. 1. While the correlation lengths are short the liquid crystal is unlikely to be strongly perturbed by the aerosil gel environment. The perturbation will only become effective when the correlation length grows to length scales comparable with the distance between gel strands. Hence the correlation length grows quickly until the disorder becomes apparent. As ρ_S increases and $\xi_\parallel$ decreases, the order parameter behavior changes from rising rapidly at low disorder to developing gradually for high gel densities. The x values inset to Fig. 6 are consistent with a gradual crossover from strongly first order to tricritical with increasing aerosil density. As shown in Table I the pseudotransition temperature, T_{IA}^*, varies little with ρ_S for 10CB-aerosil. This suggests that local variations in ρ_S are unlikely to lead to two-phase coexistence for this material. Hence the transition is not observed to be substantially smeared. The correlation length, $\overline{\xi} = (\xi_\parallel \xi_\perp^2)^{1/3}$, is characterizing short-range SmA domains within a predominantly SmA sample.

Here we are interpreting our results as if two-phase coexistence over a range of temperatures were not an important issue. This is because of the discontinuous behavior of $\xi_\parallel(T)$ at T_{IA}^*. By contrast, Bellini and coworkers [11] interpreted their x-ray results on an 10CB-aerogel sample in terms of coexisting phases - indeed they observed coexistence via optical microscopy. The 10CB-aerogel sample they studied had $\Phi \sim 0.79$ and $\overline{\xi} \sim 200$ Å, roughly comparable with our highest ρ_S aerosil sample. The temperature dependence of the peak intensity and correlation lengths are similar. One important and unusual feature of a fluctuation driven first order transition is that the disordered phase remains metastable at all temperatures [13, 34]. It may well be the case that this leads to the observed coexistence. This phenomena

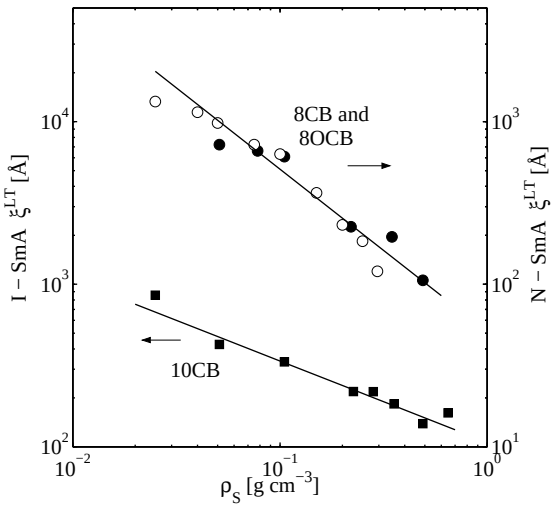

FIG. 7: A comparison of the cube root of the correlation volume, $\overline{\xi}$, taken at low temperature for 10CB-aerosil (solid squares), 8CB-aerosil [10] (open circles) and 8OCB-aerosil [20] (solid circles). The last two bulk materials have N-SmA transitions. The solid lines represent simple power law dependences, which differ for the two transitions.

is also true of the bulk material and it is unlikely to have given rise to the change in $a_2(T)$ with ρ_S that we have presented. The ratio of the volume of individual ordered domains to the volume of the complete SmA region is roughly 1:125000 and hence it is no surprise that the remaining I phase plays little role in determining $\overline{\xi}$ and only a very small role in the temperature dependence of the intensity.

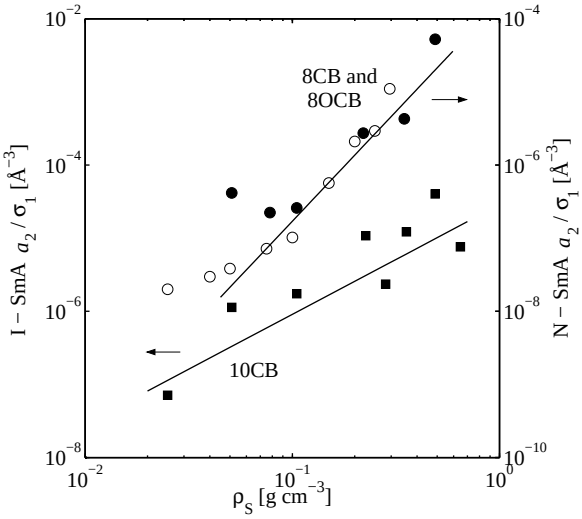

FIG. 8: A comparison of the variation of a_2/σ_1 versus ρ_S for three liquid crystal-aerosil systems at low temperatures. The symbols are the same as Fig. 7. The solid lines represent power law fits to the data described in the text. The experimental scatter is obviously large.

The observed trend in x (Fig. 6) together with previous results on other cyanobiphenyls [6, 20, 29] suggests that the disorder introduces a systematic change in transition properties. For 8CB-aerosil [6, 29] and other N-SmA transitions the aerosils change the transition characteristics away from an anisotropic critical point and toward 3D-XY behavior. The liquid crystal begins to behave as though the N order parameter is becoming increasingly saturated. Here 10CB-aerosil appears to move toward tricritical properties ($x \sim 0.5$) as aerosil is added. For the isotropic - nematic - smectic-A phase diagram this change is also equivalent to a shift toward the regime where the N phase is stable. For 8CB-aerosil and 10CB-aerosil the disorder has some effects which are equivalent to shortening the length of the molecule.

Up to this point the response of the I-SmA transition to the aerosil gel is very similar to that of the N-SmA transition in aerosil gels [20, 29]. However, Figs. 7 and 8 show that there are systematic differences in the ρ_S dependence for $\overline{\xi}$ and a_2/σ_1 associated with these two transitions. In the case of N-SmA, it was argued that ρ_S, the mass of aerosil divided by the volume of liquid crystal, corresponds to the variance of the random field [10, 19]. The dependence of $\overline{\xi}$ and a_2/σ_1 on the random field variance Δ has been determined by Aharony and Pytte [19, 35]

$$\overline{\xi} \sim \Delta^{\frac{-1}{d_\ell - d}} \tag{4}$$

$$a_2/\sigma_1 \sim \Delta^{\frac{3}{d_\ell - d}} \tag{5}$$

where d_ℓ is the lower marginal dimensionality in the presence of random fields. For transitions which break a continuous symmetry, random fields are found to shift the lower marginal dimensionality to two higher dimensions. For experimentally achievable resolutions the N-SmA transition has 3D-XY characteristics, hence $d_\ell = 4$. This is in full agreement with results for 8CB-aerosil [10] and 8OCB-aerosil [20] as shown in Figs. 7 and 8. These log-log plots strongly suggest that $d_\ell = 5$ for 10CB-aerosil. Two-phase coexistence on the scale of the individual ordered domains is predicted to give rise to more abrupt domain walls than occur within an $n \geq 2$ single-phase sample [22]. By the Imry-Ma argument [21] this would tend to reduce d_ℓ below 4. This is the opposite trend to our observations.

The observed $d_\ell = 5$ appears consistent with the absence of the orientationally ordered N phase. The formation of SmA order in 10CB gives rise to nematic order and hence the director is constrained to lie along the layer normal. Director fluctuations no longer influence the range of smectic correlations. As a result the line shape has the form anticipated for the Landau-Peierls instability Eq.(2) albeit with finite-range order. This is consistent with the use of Eq.(2) as the thermal structure factor for Eq.(3) and its square as the random-field term. The lower marginal dimensionality is general for a transition from a uniform phase to one with translational order in a single direction. Golubović and Kulić [36] have made a theoretical analysis of a similar random-field problem. They studied a system with a continuous set of energy minima in q-space, having the form of a ring as opposed to the sphere for the I-SmA transition. Following Imry and Ma [21] they determined the dimensionalities for which the correlation function for transverse fluctuations of the order parameter would diverge. The lower marginal dimensionality depends on how the inverse susceptibility varies with the wave vector. For the XY model the inverse susceptibility varies quadratically with the wave vector components [21]. For a ring of energy minima the inverse susceptibility varies quartically with one of the wave vector components and quadratically with the others [36]. For a sphere of energy minima the inverse susceptibility varies quartically with two of the components and quadratically with the others. For $d \leq d_\ell$ the correlation function in the presence of quenched random fields diverges and in these cases $d_\ell = 4, 4.5, 5$ respectively [21, 36].

The series of studies on 8CB-aerosil [6, 10, 19, 29], 8OCB-aerosil [20] and 10CB-aerosil samples provide a detailed picture of the effect of quenched random fields on the formation of the SmA phase. The first two examples relate to the case where an orientationally ordered (N) phase intervenes between the I and the SmA while the results presented here relate to the direct transition from I to SmA. The interaction between nematic fluctuations away from the smectic layer normal and the SmA order results in transverse smectic correlations which die out with $q_\perp^{-2}$. Our results suggest that, at the I-SmA transition, the molecules are constrained to be perpendicular to the layers and hence the SmA correlations die out with $q_\perp^{-4}$. There is a concomitant change in the lower marginal dimensionality. We have presented high resolution x-ray diffraction results for 10CB-aerosil samples with a range of gel densities. We have shown that an aerosil gel perturbs the I-SmA transition as though it were a random field pinning the phase of the density wave. The transition remains first order for all gel densities studied while the line shape and correlation length evolve systematically. The line shape analysis reveals reasonable agreement with a Landau-Peierls system with quenched random fields. It would be of very great interest to study the effect of aerosils at the tricritical point close to the boundary between N-SmA and I-SmA regimes.

V. ACKNOWLEDGMENTS

Funding in Toronto was provided by the Natural Science and Engineering Research Council. The National Synchrotron Light Source, Brookhaven National Laboratory, is supported by the US Department of Energy under Contract No. DE-AC02-98CH10886.

[1] R.E. Peierls, Helv. Phys. Acta Suppl. **7**, 81 (1934).
[2] L.D. Landau and E.M. Liftshitz, *Statistical Physics*, 2nd ed. (Pergamon Press, New York, 1980).
[3] C.W. Garland and G. Nounesis, Phys. Rev. E **49**, 2964 (1994) and references cited therein.
[4] D.R. Nelson and J. Toner, Phys. Rev. B **24**, 363 (1981) and references cited therein.
[5] L. Wu, B. Zhou, C.W. Garland, T. Bellini, and D.W. Schaefer, Phys. Rev. E **51**, 2157 (1995).
[6] G.S. Iannacchione, C.W. Garland, J.T. Mang, and T.P. Rieker, Phys. Rev. E **58**, 5966 (1998).
[7] H. Zeng, B. Zalar, G.S. Iannacchione, and D. Finotello, Phys. Rev. E **60**, 5607 (1999).
[8] T. Jin and D. Finotello, Phys. Rev. Lett. **86**, 818 (2001).
[9] T. Bellini, L. Radzihovsky, J. Toner, and N.A. Clark, Science **294**, 1074 (2001).
[10] R.L. Leheny, S. Park, R.J. Birgeneau, J.-L. Gallani, C.W. Garland, and G.S. Iannacchione, Phys. Rev. E **67**, 011708 (2003).
[11] T. Bellini, N.A. Clark, and D.R. Link, J. Phys.: Condens. Matter **15**, S175 (2003).
[12] P.G. de Gennes and J. Prost, *The Physics of Liquid Crystals*, 2nd ed. (Oxford University Press, New York, 1993).
[13] S.A. Brazovskii, Sov. Phys. JETP **41**, 85 (1975).
[14] M.A. Anisimov, *Critical Phenomena in Liquids and Liquid Crystals* (Gordon and Breach, Philadelphia, 1991).
[15] H. Marynissen, J. Thoen, and W. Van Dael, Mol. Cryst. Liq. Cryst., **97**, 149 (1983).
[16] The I-SmA first-order latent heat for 10CB is 2830 ± 50 J mol^{-1} and the integrated area of the pretransitional C_p wings above and below T_{IA} is only $\sim 275 \pm 100$ J mol^{-1}. J. Thoen (private communication).
[17] A. Gohin, C. Destrade, H. Gasparoux, and J. Prost, J. Phys. (France), **44**, 427 (1983).
[18] J. Thoen, H. Marynissen, and W. Van Dael, Phys. Rev. Lett. **52**, 204 (1984).
[19] G.S. Iannacchione, S. Park, C.W. Garland, R.J. Birgeneau, and R.L. Leheny, Phys. Rev. E **67**, 011709 (2003).
[20] P.S. Clegg, C. Stock, R.J. Birgeneau, C.W. Garland, A. Roshi, and G.S. Iannacchione, Phys. Rev. E **67**, 021703 (2003).
[21] Y. Imry and S.-K. Ma, Phys. Rev. Lett. **35**, 1399 (1975).
[22] Y. Imry and M. Wortis, Phys. Rev. B **19**, 3580 (1979).
[23] B.M. Ocko, R.J. Birgeneau, J.D. Litster, and M.E. Neubert, Phys. Rev. Lett. **52**, 208 (1984).
[24] J. Als-Nielsen, J.D. Litster, R.J. Birgeneau, M. Kaplan, C.R. Safinya, A. Lindegaard-Andersen, and S. Mathiesen, Phys. Rev. B **22**, 312 (1980).
[25] J.D. Litster, R.J. Birgeneau, M. Kaplan, C.R. Safinya, and J. Als-Nielsen, in *Ordering in Strongly Fluctuating Condensed Matter Systems*, edited by T. Riste (NATO ASI, Volume 50, 1979).
[26] A. Caillé, C. R. Acad. Sci. Ser. B **274**, 891 (1972).
[27] H.J. Coles and C. Strazielle, Mol. Cryst. Liq. Cryst. **49**, 259 (1979).
[28] Degussa Corp., Silica Devision, 65 Challenger Road, Ridgefield Park, NY 07660.
[29] S. Park, R.L. Leheny, R.J. Birgeneau, J.-L.Gallani, C.W. Garland, and G.S. Iannacchione, Phys. Rev. E **65**, 050703(R) (2002).
[30] BDH, Product Information (1986).
[31] P.S. Clegg, R.J. Birgeneau, S. Park, C.W. Garland, G.S. Iannacchione, R.L. Leheny, and M.E. Neubert, Phys. Rev. E **68**, 031706 (2003).
[32] Recent studies by Leheny and coworkers show that, for anisotropic 8CB-aerosil and $\overline{8}S5$-aerosil gels, the relationships $\xi_\perp(\xi_\parallel)$ and $c(\xi_\parallel)$ change compared to those for the pure liquid crystal materials. The same type of variation, if it were to occur here, would give rise to very subtle changes in parameter values.
[33] B.M. Ocko, Ph.D. thesis, Massachusetts Institute of Technology, 1984 (unpublished).
[34] G.H. Fredrickson and K. Binder, J. Chem. Phys. **91**, 7265 (1989).
[35] A. Aharony and E. Pytte, Phys. Rev. B, **27**, 5872 (1983).
[36] L. Golubović and M. Kulić, Phys. Rev. B **37**, 7582 (1988).